16th International Conference on Machine Vision Applications (MVA)
National Olympics Memorial Youth Center, Tokyo, Japan, May 27-31, 2019.

Accurate Ellipse Extraction in Low-Quality Images

Zezhong Xu
Changzhou Institute of Technology
no. 666 Liaohe Road, Changzhou, China.
xuzz@czu.cn

Cheng Qian
Changzhou Institute of Technology
no. 666 Liaohe Road, Changzhou, China.
qianc@czu.cn

Shibo Xu
Changsha High-tech Engineering School
no. 607 Dongfang Road, Changsha, China.
1744424368@qq.com

Reinhard Klette
Auckland University of Technology
Auckland, New Zealand
rklette@aut.ac.nz

Abstract

We propose an efficient method for extracting parameters of elliptic regions in digital images. Only one 2-dimensional accumulator array $A(\rho, \theta)$ is used for Hough voting, defined by voting angle θ and voting distance ρ. For each voting angle θ, the voting distance ρ is considered to be a stochastic variable, where voting values $A(\rho, \theta)$ define the probabilistic weights.

We state how the statistical variance is related to the major axis, minor axis, and direction of an elliptic region, and also how the statistical mean is related to the centre; we provide two relationship functions in image space. After voting, a linear function and a quadratic function are fitted in the parameters space. The major axis, minor axis and direction are computed based on the coefficients of the fitted quadratic function. The centre is determined by using the coefficients of the fitted linear function.

The proposed method is tested on synthetic images and real-world images. Experimental results show that the method extracts accurately parameters of elliptic regions, even in noisy and low-resolution images.

1 Introduction

An accurate extraction of ellipse parameters in real images is a challenge due to the presence of image noise, shape defects, edge blurring, or poor resolution [1, 2, 3]. For example, Fig. 1 shows on the left an image of a human's pupil recorded by a special infrared CCD video camera [4]; on the right, two extracted ellipses are shown; a pupil is more accurately approximated by an ellipse rather than just by a circle.

Many methods for ellipse extraction have been proposed [5]. These methods can be categorized into three types of approaches: Least-square fitting techniques, Hough-transform methods, or edge-following algorithms.

Least-square fitting methods are based on a minimisation between contour points and an elliptic hypothesis [6, 7, 8, 9], including algebraic fitting, orthogonal least-square fitting, or maximum-likelihood estimations. Fitting algorithms are sensitive to noise, but may be successful for only partially visible elliptic contours.

Hough-transform (HT) methods map the ellipse-extraction problem into a peak-seeking problem in parameter space. A base-line HT for ellipse extraction applies a *5-dimensional* (5D) parameter space. This implies excessive computation and storage requirements. A large diversity of variants has been proposed to improve the performance of the base-line HT for ellipse extraction.

A randomized Hough transform selects randomly groups of 3 or 5 non-collinear points to vote for cells in parameter space [10, 11]. The randomized HT reduces the computation time. It still uses a 5D accumulator array.

Geometric properties of the ellipse are exploited to reduce the dimension of the parameter space [12, 13, 14]. Due to results obtained, it appears difficult to extract accurately geometric properties when following this direction in noisy images or for cases of defective

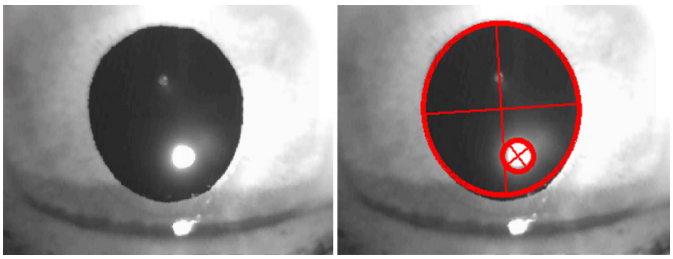

Figure 1. Extracted ellipses for an image of a human's pupil; the larger one supports an accurate measurement of the size of the pupil.

ellipses.

Edge-following methods detect arc segments [15, 16], then group those segments into elliptic arcs [17, 18], and fit an ellipse to the arcs. Edge-following methods are time-efficient. They depend on the quality of detected arcs, and they do not work well in cases of defective ellipses.

In order to extract parameters of elliptic regions in a low-quality image, this paper outlines a novel method for ellipse extraction. We only use a 2D parameter space for Hough voting. The dimensions of this Hough space are defined by voting angle and voting distance. The voting distance is considered to be a stochastic variable. We compute the statistical mean and the variance for this variable, for different voting angles. The ellipse parameters are extracted by fitting a linear function and a quadratic function to the computed statistical characteristics.

The remainder of the paper is organized as follows. Section 2 describes the Hough voting and the probabilistic distribution of voting distances. Section 3 presents the parameter-extraction technique of an elliptic region by fitting two functions. Section 4 tests the proposed methods by providing experimental results. Section 5 is our conclusion.

2 Voting Analysis

Instead of a 5D accumulator array, we only use a 2D array, with dimensions defined by voting distance ρ and voting angle θ, as already well-known from the extraction of line segments or linear regions in images.

2.1 Hough Voting

A point (x, y) in the image space votes for a *sine*-curve in the 2D parameter space using the following equation

$$\rho = x \cdot \cos\theta + y \cdot \sin\theta \tag{1}$$

For every pixel in the region of interest in the image space, the voting distances ρ with respect to different voting angles θ are computed, and corresponding cells are voted for in the 2D accumulator array. Only the introduced 2D accumulator array is maintained during voting and searching.

Regarding a voting angle θ, the computed voting distance ρ ranges from ρ_1 to ρ_2. The corresponding voting value $A(\rho, \theta)$ increases from 0 to a maximum gradually, then decreases to 0 gradually. The mean voting distance m defines the maximum voting value; the centre (x_0, y_0) of the elliptic region votes for m. This is shown in Fig. 2.

For a voting angle θ, we consider the voting distance ρ as a stochastic variable. The voting values $A(\rho, \theta)$ define the probabilistic weights of this variable.

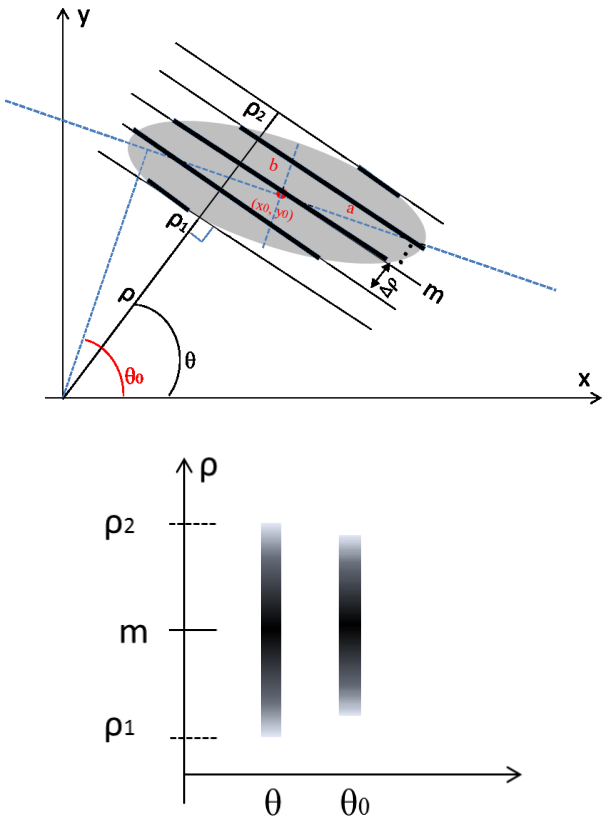

Figure 2. Voting analysis in image space and parameter space. *Top*: Voting distances ρ with respect to angle θ in image space. *Bottom*: Voting distribution of θ_0 and θ columns in parameter space; the darker the cell, the bigger is the voting value.

2.2 Probabilistic Distribution

The direction of the ellipse is supposed to be θ_0. Let the difference between θ and θ_0 be $\Delta\theta = \theta - \theta_0$, and the difference between ρ and m be $\Delta\rho = \rho - m$. In addition, S denotes $\sin\Delta\theta$ and C denotes $\cos\Delta\theta$. The voting value $A(\rho, \theta)$ of cell (ρ, θ) is given as follows:

$$A(\rho) = \frac{2ab \cdot \sqrt{a^2S^2 + b^2C^2 - \Delta\rho^2}}{a^2S^2 + b^2C^2} \tag{2}$$

with a and b defining the lengths of the axes of the elliptic region. The equation is illustrated in Fig. 3.

The voting value $A(\rho, \theta)$ is considered to be the weight. The probabilistic distribution $p(\rho)$ is defined as follows:

$$p(\rho) = \frac{A(\rho)}{\pi \cdot ab} \tag{3}$$

We analyse the statistical mean m and variance σ^2 of the voting distance ρ.

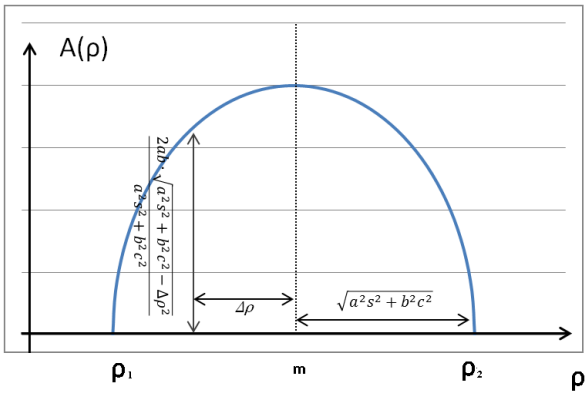

Figure 3. Probabilistic weights of voting distances.

2.3 Linear Functional Relationship

Because of the geometric symmetry of the elliptic region, the centre (x_0, y_0) contributes to the mean voting distance m.

Regarding voting angle θ, we have the following equation:

$$m = x_0 \cdot \cos\theta + y_0 \cdot \sin\theta \tag{4}$$

This equation is linearized by using the following transform:

$$m/\cos\theta = y_0 \cdot \tan\theta + x_0 \tag{5}$$

The functional relationship between $m/\cos\theta$ and $\tan\theta$ is linear.

2.4 Quadratic Functional Relationship

Based on the probabilistic distribution of the voting distance, given voting angle θ, the statistical variance σ^2 equals

$$\sigma^2 = \frac{b^2 + (a^2 - b^2)\sin^2\Delta\theta}{4} \tag{6}$$

We only consider voting angles that are close to θ_0, thus, $\sin(\Delta\theta) \approx \Delta\theta$. Therefore,

$$\begin{aligned}\sigma^2 &\approx \frac{b^2 + (a^2 - b^2)\Delta\theta^2}{4} \\ &= \frac{a^2 - b^2}{4}\theta^2 - \frac{2\theta_0(a^2 - b^2)}{4}\theta + \frac{b^2 + (a^2 - b^2)\theta_0^2}{4}\end{aligned} \tag{7}$$

The functional relationship between σ^2 and θ is a quadratic polynomial curve.

3 Ellipse Extraction

The ellipse parameters are extracted based on the statistical characteristics of columns in the parameter space.

We compute the statistical mean m and the statistical variance σ^2 of columns around a local peak. A linear function and a quadratic function are fitted next. The centre of the elliptic region is determined by the coefficients of the fitted linear function. The direction, major axis and minor axis of the elliptic region are solved using the coefficients of the fitted quadratic function.

3.1 Statistical Mean and Variance

After voting, a local peak is found in the 2D accumulator and is denoted by $(\theta_{peak}, \rho_{peak})$.

In columns θ_i, which are near θ_{peak} in the 2D accumulator array, the voting mean and variance are computed:

$$\begin{aligned} m_i &= \frac{\sum[\rho \cdot A(\rho, \theta_i)]}{\sum A(\rho, \theta_i)} \\ \sigma_i^2 &= \frac{\sum[(\rho - m_i)^2 \cdot A(\rho, \theta_i)]}{\sum A(\rho, \theta_i)} \end{aligned} \tag{8}$$

where $A(\rho, \theta_i)$ is the voting value corresponding to voting distance ρ in column θ_i.

3.2 Linear Function Fitting

Based on the statistical means m_i of columns θ_i, a linear function is fitted to the pairs $(m_i/\cos\theta_i, \tan\theta_i)$. We obtain:

$$\begin{aligned} g: \quad m/\cos\theta &= g(\tan\theta) \\ &\triangleq g_1 \cdot \tan\theta + g_0 \end{aligned} \tag{9}$$

According to Eqs. (5) and (9), the centre (x_0, y_0) of the elliptic region is as follows:

$$x_0 = g_0 \quad \text{and} \quad y_0 = g_1 \tag{10}$$

3.3 Quadratic Function Fitting

Having the statistical variance σ_i^2 of column θ_i, a quadratic function is fitted to pairs (σ_i^2, θ_i). We obtain:

$$\begin{aligned} f: \quad \sigma^2 &= f(\theta) \\ &\triangleq f_2 \cdot \theta^2 + f_1 \cdot \theta + f_0 \end{aligned} \tag{11}$$

Based on Eqs. (7) and (11), there are the following equations:

$$\begin{aligned} (a^2 - b^2)/4 &= f_2 \\ -2(a^2 - b^2)\theta_0/4 &= f_1 \\ \left(b^2 + (a^2 - b^2)\theta_0^2\right)/4 &= f_0 \end{aligned} \tag{12}$$

Table 1. Comparison of detection accuracies.

	Detection errors											
	Fitting				Edge following				2D-space HT			
	Centre	Major	Minor	Direction	Centre	Major	Minor	Direction	Centre	Major	Minor	Direction
Normal	0.04	0.04	0.02	0.04	0.76	1.12	0.45	0.74	0.04	0.67	0.02	0.10
Noise	N/A				0.92	1.29	0.60	0.75	0.55	1.46	0.35	0.94
Low resolution	2.13	0.22	0.13	0.24	N/A				2.16	0.97	0.13	0.27

By solving the above equations, the direction, major axis and minor axis are given by

$$\theta_0 = -f_1/(2f_2) \quad (13)$$

$$a = 2\sqrt{f_2 + f_0 - \frac{f_1^2}{4f_2}} \quad (14)$$

$$b = 2\sqrt{f_0 - \frac{f_1^2}{4f_2}} \quad (15)$$

4 Experimental Results

The proposed method for elliptic regions detection is tested on synthetic and real-world images.

4.1 Test on Synthetic Images

We generate randomly synthetic 500 × 400 images, each containing one elliptic region. The known parameters of the elliptic regions are recorded as ground truth.

Ellipse extraction results are compared with those of a fitting method [8] and with those of an edge-following method [17].

In order to test the robustness with respect to image noise and low resolution, noisy pixels are added, and the image is down-sampled and again up-sampled. An example of a noisy and low resolution image is shown in Fig. 4.

One hundred synthetic images (without any preprocessing) are processed using the fitting method, the edge-following method and the proposed 2D-space HT method. We compare results under different conditions. First, we consider the images without any noise (case "Normal"). Then, images are distorted by producing 2,000 noisy pixels (case "Noise"). Finally, we use a low resolution image that is down-sampled and up-sampled by factor 4 (case "Low resolution"). Mean detection errors are listed in Table 1.

All three methods can extract accurately the parameters of an elliptic region for "normal" images. The fitting method does not work well for a noisy image, and the edge-following method is not applicable for the considered low-resolution images. The 2D-space HT method can extract the elliptic region both in noisy images as well as in the considered low-resolution images.

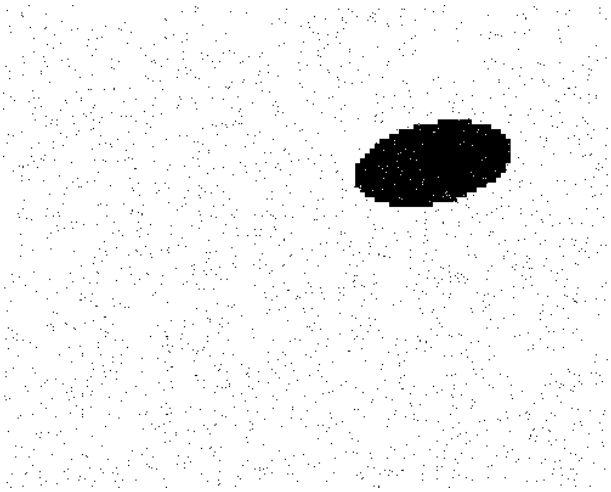

Figure 4. An example of noisy and low-resolution image with an elliptic region.

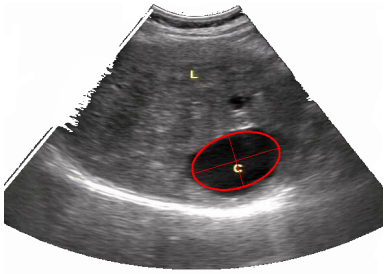

Figure 5. Extraction of an elliptic region in an image with heavy noise.

4.2 Test on Real-world Images

Figure 1 showed results when applying the proposed 2D-space HT method. We tested the proposed method also on low-quality ultrasound images.

An example of such an image with heavy noise is shown in Fig. 5. The 2D-space HT method extracts the elliptic region in spite of an obscure contour and heavy noise.

Figure 6 shows a low-resolution image after being down-sampled and up-sampled. Although the image

quality is low, the 2D space HT method can extract the elliptic region.

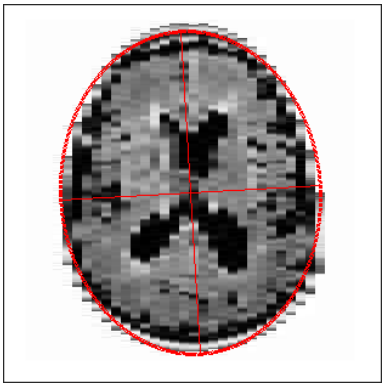

Figure 6. Extraction of an elliptic region in a low-resolution image.

5 Conclusions

This paper proposes a closed-form solution for parameters extraction of elliptic regions using a 2D Hough transform. By analysing the voting results in the Hough space, a linear function and a quadratic function are deduced. By computing means and variances of columns in parameter space, two functions are fitted. The centre of the elliptic region is calculated by the coefficients of the fitted linear function; the direction, major axis and minor axis are computed by the coefficients of the fitted quadratic function. The extracted parameters of elliptic regions are also accurate for low-quality images.

Acknowledgment

This work was supported by the National Natural Science Foundation of China (61602063), Jiangsu Collaborative Innovation Centre for Cultural Creativity (XYN1705), and Changzhou Science and Technology Project (CE20172023).

References

[1] V. Pătrăucean, P. Gurdjos, and R.G.V. Gioi, "JointA ContrarioEllipse and line detection," IEEE Trans. Pattern Analysis Machine Intelligence, vol. 39, pp. 788–802, 2017.

[2] R. Jin, H.M. Owais, T. Song, and D. Lin, "Towards fast and accurate ellipse and semi-ellipse detection," In: *IEEE Int. Conf. Image Processing*, pp. 743–747, 2018.

[3] J. Liang , Y. Wang, and X. Zeng, "Robust ellipse fitting via half-quadratic and semi-definite relaxation optimization," IEEE Trans. Image Processing, vol. 24, pp. 4276–4286, 2015.

[4] X. Lin, J.P. Craig, S.J. Dean, G. Klette, and R. Klette, "Accurately measuring the size of the pupil of the eye," Proc. Image Vision Computing New Zealand, `hdl.handle.net/2292/2840`, 2003.

[5] C.Y. Wong, S.C.F. Lin, T.R. Ren, and N.M. Kwok, "A survey on ellipse detection methods," Proc. IEEE Int. Symp. Industrial Electronics, pp. 1105–1110, 2012.

[6] D.K. Prasad, M.K. Leung, and C. Quek, "ElliFit: an unconstrained, non-iterative, least squares based geometric ellipse fitting method," Pattern Recognition, vol. 46, pp. 1449–1465, 2013.

[7] S. Mulleti and C.S. Seelamantula, "Ellipse fitting using the finite rate of innovation sampling principle," IEEE Trans. Image Processing, vol. 25, pp. 1451–1464, 2016.

[8] A. Fitzgibbon, M. Pilu, and R.B. Fisher, "Direct least square fitting of ellipses," IEEE Trans. Pattern Analysis Machine Intelligence, vol. 21, pp. 476–480, 1999.

[9] K. Kanatani, Y. Sugaya, and Y. Kanazawa, "Ellipse Fitting for Computer Vision: Implementation and Applications," Morgan & Claypool, Williston, VA, 2016.

[10] R.A. McLaughlin, "Randomized Hough transform: Improved ellipse detection with comparison," Pattern Recognition Letters, vol. 19, pp. 299–305, 1998.

[11] L. Xu, E. Oja, and P. Kultanen, "A new curve detection method: Randomized Hough transform (RHT)," Pattern Recognition Letters, vol. 11, pp. 331–338, 1990.

[12] S.C. Zhang and Z.Q. Liu, "A robust, real-time ellipse detector," Pattern Recognition, vol. 38, pp. 273–287, 2005.

[13] Y. Lei and K.C. Wong, "Ellipse detection based on symmetry," Pattern Recognition Letter, vol. 20, pp. 41–47, 1999.

[14] Y. Xie and Q. Ji, "A new efficient ellipse detection method," Proc. Int. Conf. Pattern Recognition, vol. 2, pp. 957–960, 2002.

[15] D.K. Prasad, M.K.H. Leung, and S.Y. Cho, "Edge curvature and convexity based ellipse detection method," Pattern Recognition, vol. 45, pp. 3204–3221, 2012.

[16] H. Dong, I.M. Chen, and D.K. Prasad, "Robust ellipse detection via arc segmentation and classification," Proc. IEEE Int. Conf. Image Processing, pp. 66–70, 2018.

[17] M. Fornaciari, A. Prati, and R. Cucchiara: "A fast and effective ellipse detector for embedded vision applications," *Pattern Recognition*, vol. 47, pp. 3693–3708, 2014.

[18] T.M. Nguyen, S. Ahuja, and Q.M.J. Wu, "A real-time ellipse detection based on edge grouping," Proc. IEEE Int. Conf. Systems Man Cybernetics, pp. 3280–3286, 2009.